arXiv:1610.01207v1 [nucl-th] 4 Oct 2016

MANIFESTATION OF THE *P*-WAVE DIPROTON RESONANCE IN SINGLE-PION PRODUCTION IN *pp* COLLISIONS

M. N. Platonova* and V. I. Kukulin†

Skobeltsyn Institute of Nuclear Physics,

Lomonosov Moscow State University, Moscow 119991, Russia

Abstract

It is demonstrated that many important features of single-pion production in pp collisions at intermediate energies ($T_p \simeq 400$–800 MeV) can naturally be explained by supposing excitation of intermediate diproton resonances in pp channels $^1D_2$, $^3F_3$ and $^3P_2$, in addition to conventional mechanisms involving an intermediate Δ-isobar. We predict for the first time the crucial role of the $^3P_2$ diproton resonance, found in recent experiments on the single-pion production reaction $pp \to pp(^1S_0)\pi^0$, in reproducing the proper behavior of spin-correlation parameters in the reaction $pp \to d\pi^+$ which were poorly described by conventional meson-exchange models to date. The possible quark structure of the P-wave diproton resonances is also discussed.

*Electronic address: platonova@nucl-th.sinp.msu.ru

†Electronic address: kukulin@nucl-th.sinp.msu.ru

I. INTRODUCTION. BRIEF HISTORICAL EXCURSUS

The activity in searching for dibaryon resonances in 1980s was motivated by the success of MIT-bag models in prediction of dibaryon states [1–3]. Numerous experiments on $\vec{p}\vec{p}$ elastic scattering done at the same time revealed possible existence of a series of diproton resonances with masses in the range 2.1–2.9 GeV and total widths 100–200 MeV [4–8]. Further studies established that these resonances are mainly of inelastic nature and seen primarily in inelastic channels like $pp \to d\pi^+$, $pp \to pn\pi^+$, etc. [9]. Using different data sets, a few groups performed partial-wave analyses (PWA) of pp and $\pi^+ d$ elastic scattering and the $pp \leftrightarrow d\pi^+$ reaction [10–15] and found resonance poles in the ${}^1D_2$, ${}^3F_3$, ${}^3P_2$, ${}^1G_4$ and other NN channels. However some authors suggested the observed singularities to be related to the so-called pseudoresonances (see, e.g., [16]), which means rather generation of a resonance in a subsystem instead of the true diproton resonance in a whole interacting system. In case of pp scattering at energies $T_p \simeq 600$ MeV, the pseudoresonance implies an intermediate Δ-isobar generation coupled strongly to the rest nucleon. Thus, the resonance behavior of the pp elastic and inelastic scattering amplitudes is basically associated with the nearby $N\Delta$ thresholds in the respective partial waves [17, 18]. Similar discussions about dibaryon resonances near the $\Delta\Delta$ threshold were very active for the last three decades, at least (see, e.g., [19]).

This rather indefinite situation began to change only in recent years when an experimental group using the 4π detector WASA installed at the COSY facility (Juelich) together with the SAID Data Analysis Center announced [20, 21] the discovery of an $I(J^P) = 0(3^+)$ dibaryon resonance d^* with a mass $M_{d^*} \simeq 2.38$ GeV in the ${}^3D_3$–${}^3G_3$ channels of NN system both in 2π-production reactions and $\vec{n}p$ elastic scattering. This resonance called an "inevitable dibaryon" [22] had been searched for 50 years since its first prediction by Dyson and Xuong still in 1964 [23]. Remarkably, the d^* dibaryon was predicted in [23] to belong to the same SU(3) multiplet as the deuteron — the lowest isoscalar dibaryon, while the ${}^1D_2$ dibaryon was predicted to belong to the same SU(3) multiplet as the singlet deuteron — the lowest isovector dibaryon. Very recently another experimental group which uses the forward detector ANKE at the COSY facility have received an evidence [24] of the ${}^3P_2$ and ${}^3P_0$ diproton resonances with a mass $M_D \simeq 2.2$ GeV in the reaction $pp \to (pp)_0\pi^0$, where $(pp)_0$ means the ${}^1S_0$ singlet deuteron near-threshold state.

From the theoretical side, the calculations [25, 26] within the framework of rigorous three-body πNN and $\pi N\Delta$ models revealed a robust ${}^1D_2$ dibaryon resonance pole near the $N\Delta$ threshold and also a ${}^3D_3$ resonance pole near (below) the $\Delta\Delta$ threshold. Furthermore, the recent quark model studies of the d^* dibaryon strongly support its unconventional nature as being a genuine six-quark state rather than just a Δ–Δ bound state. Indeed, the observed width and decay properties of this resonance can be explained only if one assumes that it is dominated by a "hidden-color" six-quark configuration [27–29]. The "hidden-color" six-quark states are a rigorous first-principle prediction of SU(3) color gauge theory [30, 31]. We also cite in this connection the recent issue of CERN Courier [32] in section "News. New particles": "COSY confirms existence of six-quark states". So, in light of these new findings, one may hope that the long-term dispute between the supporters of the near-threshold singularities in $N\Delta$ and $\Delta\Delta$ channels and the apologists of the true dibaryon resonances will shortly come to its completion.

If to consider the dispute between two above alternatives from the general physical point of view, we should say that as was recognized still long ago by Baz' [33] who developed Wigner's ideas [34] on the near-threshold cross section singularities in the field of nuclear reactions, there should be (in majority of nuclei) a strong correlation between the position of a threshold for some channel $B + C$ in a nucleus $A = B + C$ and the near-threshold energy levels with appropriate quantum numbers. It is because the fragments B and C can move far apart near the channel threshold keeping thereby their identity, so that, a near-threshold bound (or resonance) state should emerge very likely. A careful inspection [35] of the well-known nuclear level tables [36] actually confirmed the close correlation between the channel thresholds and the nearby bound states in many nuclei (e.g., ${}^{12}\mathrm{C}^* \to {}^8\mathrm{Be} + \alpha$, ${}^{16}\mathrm{O}^* \to {}^{12}\mathrm{C}^* + \alpha$, etc.). Hence, it can be supposed quite naturally that there is a strong correlation between thresholds and the nearby bound (or resonance) states also in hadronic physics [37, 38]. A good example may be the Roper resonance $N^*(1440)$, its average pole mass[1] being $M_{\mathrm{pole}} \simeq 1365$ MeV [40]. In fact, it has been found experimentally [41, 42] that the very large (or even dominating) decay mode for the Roper resonance is the light scalar σ-meson emission (with $m_\sigma \simeq 400$–500 MeV), so that, the Roper can be treated as a

[1] One should bear in mind that a double-pole structure with two almost degenerate poles was found for the Roper resonance in [39] and recently confirmed by ANL-Osaka and Juelich groups.

near-threshold state in the $\sigma + N$ channel [43]. The recent Faddeev calculations for "meson-assisted dibaryons" [44] seem to confirm the general correlation between thresholds and the nearby bound (or resonance) states in the dibaryon field as well.

Moreover, QCD does not forbid existence of multiquark states near thresholds or elsewhere. Recent experimental discoveries of the tetra- and pentaquarks [45, 46] have confirmed existence of exotic multiquark states in general. So, in view of all these new achievements, studying the properties of multiquark states and their manifestation in the basic hadronic processes has become of particular importance now.

The present paper is dedicated to study of manifestation of diproton (dibaryon) resonances in single-pion production in pp collisions in the GeV region. The main emphasis will be given to the basic pion-production reaction $pp \to d\pi^+$ at energies $T_p \simeq 400$–800 MeV where a few PWA as well as a rich set of experimental data exist. In the work [47] we elaborated a model which combines two dominating conventional mechanisms of this reaction, i.e., one-nucleon exchange and an intermediate Δ excitation, with the resonance mechanisms based on intermediate dibaryons excitation. By re-examining the conventional Δ-excitation mechanism, we have shown its strong sensibility to the short-range cut-off parameters Λ in meson-baryon vertices, especially in the $\pi N\Delta$ vertex. Thus, when using "soft" cut-off parameters which naturally arise from description of πN elastic scattering in the Δ region, the conventional meson-exchange mechanisms give a strong underestimation for the partial and total $pp \to d\pi^+$ cross sections. So, we have shown that the significant contribution should come from other sources (of the short-range nature), and that excitation of intermediate dibaryons in the dominant partial waves ${}^1D_2P$ and ${}^3F_3D$ of the reaction $pp \to d\pi^+$ can really give this lacking contribution.

To our knowledge, the only attempt (besides the PWA) to describe the reaction $pp \to d\pi^+$ at energies $T_p \simeq 400$–800 MeV including dibaryon resonances was made previously in the works [48, 49]. The authors used essentially the same model as we did in [47], but with a more sophisticated treatment of $NN \to N\Delta$ amplitudes, and came to a conclusion similar to ours, that the conventional mechanisms give only a half of the total cross section. Then, by fitting the parameters of six hypothetical dibaryon resonances to the existing experimental data, they also revealed importance of two dibaryon resonances, ${}^1D_2$ and ${}^3F_3$, in reproducing the total and differential cross sections and also the proton analyzing power. However, the masses of resonances other than ${}^1D_2$ and ${}^3F_3$ were found in their analysis to be too low,

and their widths too narrow. Besides that, their model calculations could not reproduce the spin-correlation parameters properly. On the contrary, we fit the results of the most recent PWA [50, 51] rather than experimental data, and include dibaryons only in three dominant partial waves, ${}^1D_2P$, ${}^3F_3D$ and (in the present paper) ${}^3P_2D$, where the resonance behavior of the amplitudes is well established. Thus, we can extract the dibaryon parameters more precisely and judge on the role of individual resonances in $pp \to d\pi^+$ observables.

In the present study, we focus on differential observables of the reaction $pp \to d\pi^+$ and on the role of the P-wave diproton resonance which can be excited in the ${}^3P_2D$ partial wave of the reaction. The ${}^3P_2$ diproton resonance found previously in the PWA of pp elastic scattering [52, 53] and confirmed in a recent experiment on the reaction $pp \to (pp)_0\pi^0$ [24] received much less attention in literature than the ${}^1D_2$ and ${}^3F_3$ resonances. As we will show in the paper, the ${}^3P_2$ dibaryon, though giving a small contribution ($< 10\%$) to the total $pp \to d\pi^+$ cross section, is very important for reproducing the differential observables, especially spin-correlation parameters, which have been poorly described by the conventional meson-exchange models up to date [54–56] and also by a model [48, 49] which included dibaryon resonances.

The structure of the paper is following. In Sect. II the working model for treatment of the reaction $pp \to d\pi^+$ with both intermediate Δ's and dibaryons is formulated. In Sect. III the description of the partial cross sections in the dominant partial waves ${}^1D_2P$, ${}^3F_3D$ and ${}^3P_2D$ and also of the total cross section in a broad energy range is given. Sect. IV is devoted to discussion of differential cross section, as well as vector analyzing powers and spin-correlation parameters, at energy $T_p = 582$ MeV. In Sect. V the basic results attained in the paper are summarized and discussed.

II. THEORETICAL MODEL

In this section, we briefly outline our model formalism for the reaction $pp \to d\pi^+$. The details can be found in Ref. [47]. The model includes three basic mechanisms depicted in Fig. 1. Two conventional mechanisms, i.e., one-nucleon exchange and excitation of the intermediate $N\Delta$ system by the t-channel pion exchange are shown in Figs. 1 (a) and (b), respectively. Further on, we will refer to these mechanisms as ONE and $N\Delta$. An excitation of the intermediate Δ isobar through the ρ-meson exchange was also often considered in

the literature [57], but such a mechanism contributes significantly only when choosing very high cut-off parameters in the meson-baryon form factors. Here, we choose the low values for the cut-off parameters $\Lambda < 1$ GeV (reasons for this will be given below), for which the contribution of the ρ-exchange mechanism is very small.

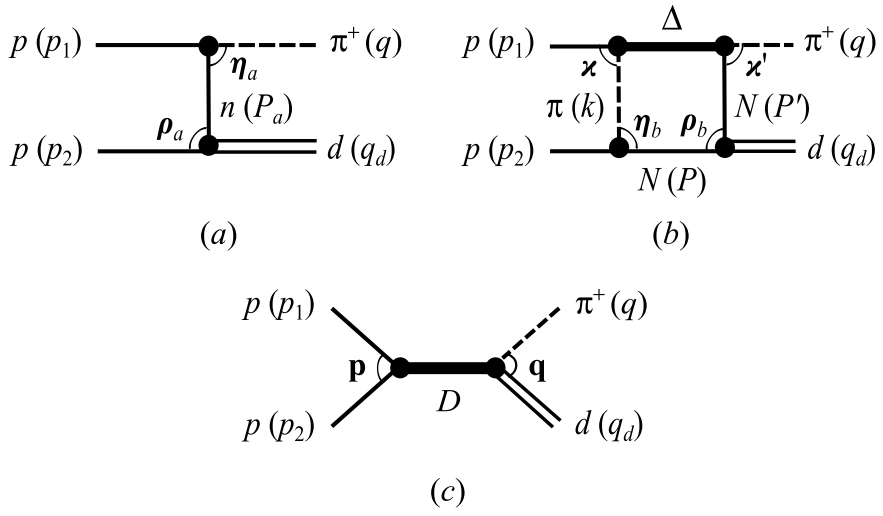

FIG. 1: Diagrams illustrating three basic mechanisms for the reaction $pp \to d\pi^+$: one-nucleon exchange (a), intermediate Δ-isobar excitation (b), and intermediate dibaryon resonance excitation (c). The 4-momenta of the particles are shown in parentheses, and 3-momenta in pair center-of-mass systems are denoted by bold face.

In a standard approximation of the spectator nucleon [57], the helicity amplitudes corresponding to the mechanisms ONE and $N\Delta$ take the form:

$$\mathcal{M}^{(\mathrm{ONE})}_{\lambda_1,\lambda_2;\lambda_d} = -\sqrt{2}(2m)^{3/2}\chi^\dagger(\lambda_2) i\sigma_2 \times \Psi^*_d(\boldsymbol{\rho_a},\lambda_d) F_{\pi NN}(\eta_a)(\boldsymbol{\sigma\eta_a})\chi(\lambda_1), \tag{1}$$

$$\mathcal{M}^{(N\Delta)}_{\lambda_1,\lambda_2;\lambda_d} = -4\sqrt{2}/3(2m)^{1/2}\chi^\dagger(\lambda_2) i\sigma_2 \int \frac{d^3P}{(2\pi)^3} \frac{F_{\pi NN}(\eta_b)(\boldsymbol{\sigma\eta_b})}{w_\pi^2 - m_\pi^2 + i0}$$

$$\times \Psi^*_d(\boldsymbol{\rho_b},\lambda_d) \sqrt{\frac{\Gamma_\Delta(\varkappa)\Gamma_\Delta(\varkappa')}{\varkappa^3\varkappa'^3}} \frac{16\pi W_\Delta^2 (\boldsymbol{\varkappa\varkappa'} + i\frac{\boldsymbol{\sigma}}{2}\boldsymbol{\varkappa}\times\boldsymbol{\varkappa'})}{W_\Delta^2 - M_\Delta^2 + iW_\Delta\Gamma_\Delta(W_\Delta)}\chi(\lambda_1), \tag{2}$$

where $w_\pi^2 = k^2$, and the Δ-isobar width is related to the vertex function $F_{\pi N\Delta}$ as

$$\Gamma_\Delta(\varkappa) = \frac{\varkappa^3 m}{6\pi W_\Delta} F^2_{\pi N\Delta}(\varkappa). \tag{3}$$

To calculate the spin structure of the amplitudes, it is convenient to write the deuteron wave function as

$$\Psi_d(\boldsymbol{\rho},\lambda_d) = \boldsymbol{\sigma}\mathbf{E}(\boldsymbol{\rho},\lambda_d), \tag{4}$$

where we introduced the vector

$$\mathbf{E}(\boldsymbol{\rho},\lambda_d)=u(\rho)\boldsymbol{\varepsilon}(\lambda_d)+\frac{w(\rho)}{\sqrt{2}}\left(\boldsymbol{\varepsilon}(\lambda_d)-\frac{3\boldsymbol{\rho}(\boldsymbol{\rho}\boldsymbol{\varepsilon}(\lambda_d))}{\rho^2}\right). \tag{5}$$

Here, $\boldsymbol{\varepsilon}(\lambda_d)$ is the standard deuteron polarization vector, u and w are the S- and D-wave components of the d.w.f. normalized as $\int d^3\rho\,(u^2+w^2)\,/(2\pi)^3=1$.

The helicity amplitudes antisymmetrized over two initial protons take the form

$$\mathcal{M}^{(s)}_{\lambda_1,\lambda_2;\lambda_d}(\theta)=\mathcal{M}_{\lambda_1,\lambda_2;\lambda_d}(\theta)\,+\,(-1)^{\lambda_d}\mathcal{M}_{\lambda_2,\lambda_1;\lambda_d}(\pi-\theta). \tag{6}$$

Overall, there are 6 independent helicity amplitudes in the reaction $pp\to d\pi^+$ [56]:

$$\begin{aligned}\Phi_1&=\mathcal{M}^{(s)}_{\frac{1}{2},\frac{1}{2};1},\quad \Phi_2=\mathcal{M}^{(s)}_{\frac{1}{2},\frac{1}{2};0},\quad \Phi_3=\mathcal{M}^{(s)}_{\frac{1}{2},\frac{1}{2};-1},\\ \Phi_4&=\mathcal{M}^{(s)}_{\frac{1}{2},-\frac{1}{2};1},\quad \Phi_5=\mathcal{M}^{(s)}_{\frac{1}{2},-\frac{1}{2};0},\quad \Phi_6=\mathcal{M}^{(s)}_{\frac{1}{2},-\frac{1}{2};-1}.\end{aligned} \tag{7}$$

For comparison of the theoretical results with the PWA data and for studying the contributions of the intermediate dibaryon resonances, it is convenient to deal with the partial-wave amplitudes, which are expressed through the helicity ones via the standard formulas given by Jacob and Wick [58]. The dominant partial-wave amplitudes in a broad energy range including the region of Δ excitation, as was shown by $\pi^+d\to pp$ PWA (see, e.g., Fig. 5b in Ref. [50]), are ${}^1D_2P$, ${}^3F_3D$ and ${}^3P_2D$ (with decreasing magnitude). The explicit formulas for these amplitudes are

$$A({}^1D_2P)=\frac{1}{2}\sqrt{\frac{3}{5}}\left(\Phi_1^{(2)}+\Phi_3^{(2)}\right)+\frac{1}{\sqrt{5}}\Phi_2^{(2)}, \tag{8}$$

$$A({}^3F_3D)=-\frac{2}{\sqrt{7}}\Phi_4^{(3)}-\frac{1}{2}\sqrt{\frac{6}{7}}\Phi_5^{(3)}, \tag{9}$$

$$A({}^3P_2D)=\sqrt{\frac{1}{10}}\left(\Phi_1^{(2)}-\Phi_3^{(2)}\right)+\sqrt{\frac{3}{5}}\Phi_4^{(2)}, \tag{10}$$

where

$$\Phi_i^{(J)}=\int\limits_{-1}^{1}d^{(J)}_{\lambda_1-\lambda_2,-\lambda_d}(x)\Phi_i(x)dx,\quad x=\cos(\theta). \tag{11}$$

For the amplitude corresponding to excitation of an intermediate dibaryon resonance (see Fig. 1(c)), it is convenient to start from the partial-wave representation. The respective amplitude is

$$A^{(D)}({}^{2S+1}L_JL_\pi)=-\frac{8\pi s}{\sqrt{pq}}\frac{\sqrt{2\Gamma_i(s)\,\Gamma_f(s)}}{s-M_D^2+i\sqrt{s}\Gamma_D(s)}, \tag{12}$$

where $p = (s - 4m^2)^{1/2}/2$ and $q = \left[(s - m_\pi^2 - m_d^2)^2 - 4m_\pi^2 m_d^2\right]^{1/2}/2\sqrt{s}$ are the moduli of the proton and the pion c.m.s. momenta, respectively. The factor 2 before the incoming width $\Gamma_i(s)$ was introduced to account for two identical protons in the initial state.

For the incoming width $\Gamma_i(s) \equiv \Gamma_{D\to pp}(s)$, we used the Gaussian parameterization which follows from the $D \to NN$ form factor parameterization employed in the dibaryon model for NN interaction [59, 60]:

$$\Gamma_i(s) = \Gamma_i \left(\frac{p}{p_0}\right)^{2L+1} \exp\left(-\frac{p^2 - p_0^2}{\alpha_{pp}^2}\right), \tag{13}$$

where p_0 is the value of the pp relative momentum at $\sqrt{s} = M_D$.

For the outgoing width $\Gamma_f(s) \equiv \Gamma_{D\to\pi^+ d}(s)$, we employed the parameterization analogous to that for the $\Delta \to \pi N$ width (cf. (3) with a monopole form factor (25)):

$$\Gamma_f(s) = \Gamma_f \left(\frac{q}{q_0}\right)^{2L_\pi+1} \left(\frac{p_0^2 - \Lambda_{\pi d}^2}{p^2 - \Lambda_{\pi d}^2}\right)^{L_\pi+1}, \tag{14}$$

where q_0 is the value of the πd relative momentum at $\sqrt{s} = M_D$. This parameterization was proposed for πN and KN elastic scattering still in [61, 62] and then applied for the $\pi^+ d \to pp$ PWA in [13]. The same energy dependence was assumed here also for the total dibaryon width $\Gamma_D(s)$, since, due to the high inelasticity of dibaryon resonances, the incoming width $\Gamma_{D\to pp}$ is only a small fraction (ca. 10%) of the total width [18].

By using Eq. (12) and the Jacob–Wick formulas [58] which are an inversion of Eqs. (8)–(10), one can find the contributions from intermediate dibaryons to the helicity amplitudes Φ_i $(i = 1, \ldots 6)$. One should also note that $\Phi_6^{(J)} = \Phi_4^{(J)}$ for odd J and $\Phi_6^{(J)} = -\Phi_4^{(J)}$ for even J [56]. Then the respective helicity amplitudes, when three dibaryon resonances are taken into account, take the form

$$\Phi_1^{(D)} = \left(\frac{\sqrt{15}}{2} A^{(D)}({}^1D_2P) + \sqrt{\frac{5}{2}} A^{(D)}({}^3P_2D)\right) d^{(2)}_{0,-1}(x),$$

$$\Phi_2^{(D)} = \sqrt{5} A^{(D)}({}^1D_2P)\, d^{(2)}_{0,0}(x),$$

$$\Phi_3^{(D)} = \left(\frac{\sqrt{15}}{2} A^{(D)}({}^1D_2P) - \sqrt{\frac{5}{2}} A^{(D)}({}^3P_2D)\right) d^{(2)}_{0,1}(x),$$

$$\Phi_4^{(D)} = -\sqrt{7} A^{(D)}({}^3F_3D) d^{(3)}_{1,-1}(x) + \frac{\sqrt{15}}{2} A^{(D)}({}^3P_2D) d^{(2)}_{1,-1}(x),$$

$$\Phi_5^{(D)} = -\sqrt{\frac{21}{2}} A^{(D)}({}^3F_3D)\, d^{(3)}_{1,0}(x),$$

$$\Phi_6^{(D)} = -\sqrt{7}A^{(D)}({}^3F_3D)d^{(3)}_{1,1}(x) - \frac{\sqrt{15}}{2}A^{(D)}({}^3P_2D)d^{(2)}_{1,1}(x). \tag{15}$$

One can see that the ${}^1D_2P$ amplitude gives the dominant contribution to the helicity amplitudes Φ_1–Φ_3, while the ${}^3F_3D$ amplitude gives the dominant contribution to Φ_4–Φ_6. At the same time, the ${}^3P_2D$ amplitude introduces corrections to both sets of helicity amplitudes. As will be shown in Sect. IV, these corrections, though being rather small in magnitude, turn out to be crucial for polarization observables in the $pp \to d\pi^+$ reaction.

The partial cross sections are expressed through the partial-wave amplitudes as follows:

$$\sigma({}^{2S+1}L_JL_\pi) = \frac{(2J+1)}{64\pi s}\frac{q}{p}\left|A({}^{2S+1}L_JL_\pi)\right|^2. \tag{16}$$

Further, we give the expressions for observables in terms of six helicity amplitudes Φ_i ($i = 1, \ldots 6$), using the notations of Ref. [56] (apart from a $2m$ factor in the amplitudes normalization), with the signs of polarization observables given in Madison convention. A different notation for amplitudes and observables can be found in, e.g., [50].

For the total cross section, one has

$$\sigma(pp \to d\pi^+) = \frac{1}{64\pi s}\frac{q}{p}\int\limits_{-1}^{1}\sum_{i=1}^{6}\left|\Phi_i(x)\right|^2 dx. \tag{17}$$

The following expressions hold for the differential cross section:

$$\frac{d\sigma}{d\Omega}(pp \to d\pi^+) = \frac{1}{64\pi^2 s}\frac{q}{p}\frac{1}{4}\Sigma, \quad \Sigma = 2\sum_{i=1}^{6}\left|\Phi_i\right|^2, \tag{18}$$

for proton and deuteron vector analyzing powers:

$$A_{y0} = 4\mathrm{Im}\left(\Phi_1^*\Phi_6 + \Phi_3^*\Phi_4 - \Phi_2^*\Phi_5\right)\Sigma^{-1}, \tag{19}$$

$$iT_{11} = -\sqrt{6}\mathrm{Im}\left[\left(\Phi_1^* - \Phi_3^*\right)\Phi_2 + \left(\Phi_4^* - \Phi_6^*\right)\Phi_5\right]\Sigma^{-1}, \tag{20}$$

and for proton-proton spin-correlation parameters:

$$A_{xx} = \left[4\mathrm{Re}\left(\Phi_1^*\Phi_3 - \Phi_4^*\Phi_6\right) + 2\left|\Phi_5\right|^2 - 2\left|\Phi_2\right|^2\right]\Sigma^{-1}, \tag{21}$$

$$A_{yy} = \left[4\mathrm{Re}\left(\Phi_1^*\Phi_3 + \Phi_4^*\Phi_6\right) - 2\left|\Phi_5\right|^2 - 2\left|\Phi_2\right|^2\right]\Sigma^{-1}, \tag{22}$$

$$A_{zz} = -2\left(\left|\Phi_1\right|^2 + \left|\Phi_2\right|^2 + \left|\Phi_3\right|^2 - \left|\Phi_4\right|^2 - \left|\Phi_5\right|^2 - \left|\Phi_6\right|^2\right)\Sigma^{-1}, \tag{23}$$

$$A_{xz} = 4\mathrm{Re}\left(\Phi_1^*\Phi_6 + \Phi_3^*\Phi_4 - \Phi_2^*\Phi_5\right)\Sigma^{-1}. \tag{24}$$

There are also deuteron tensor analyzing powers and spin-correlation parameters for proton and deuteron and two protons and deuteron [50, 56]. However, experimental data exist for the above-defined observables only, so, in the present paper, we restrict our calculations to these observables.

The meson-baryon vertex functions $F_{\pi NN}$ and $F_{\pi N\Delta}$ were parameterized in a monopole form[2]

$$F_{\pi NN}(p,\tilde{\Lambda}) = \frac{f}{m_\pi}\frac{p_0^2+\tilde{\Lambda}^2}{p^2+\tilde{\Lambda}^2}, \quad F_{\pi N\Delta}(p,\tilde{\Lambda}_*) = \frac{f_*}{m_\pi}\frac{p_0^2+\tilde{\Lambda}_*^2}{p^2+\tilde{\Lambda}_*^2}, \tag{25}$$

where p^2 is a modulo squared of the π–N relative momentum (i.e., the pion momentum in the πN c.m.s.) and p_0^2 corresponds to the situation when all three particles are real, i.e., located on their mass shells (so, p_0^2 is positive for $\pi N\Delta$ and negative for πNN vertex). The coupling constants in Eq. (25) have been taken to be $f = 0.97$ and $f_* = 2.17$. In this case, one has $f^2/4\pi = 0.075$, and the above value for f_* was derived from the total width of the Δ isobar $\Gamma_\Delta = 117$ MeV as given by the Particle Data Group [40].

As was argued in [47], the main advantage of the above vertex parametrization is that it admits a straightforward off-shell continuation and describes the real and virtual particles *in a unified manner*. It does not require introducing any additional parameters to account for the particles leaving their mass shells. Hence, it can be used for consistent description of processes involving on- and off-shell pions, i.e., $\pi N \to \pi N$, $NN \to \pi d$, elastic NN scattering, etc., with the same cut-off parameters in meson-baryon vertices. Moreover, the cut-off parameters Λ in such a case do not need to be fitted *ad hoc* and can in general be found directly from experimental data.

Thus, the parameter $\tilde{\Lambda}_*$ in the $\pi N\Delta$ vertex can be found from empirical data on πN elastic scattering. From fitting the PWA (SAID) data [63] for the πN-scattering P_{33} partial cross section in a broad energy range within the isobar model, we found $\tilde{\Lambda}_* = 0.3$ GeV (see Fig. 2). For the πNN vertex, we have chosen the value $\tilde{\Lambda} = 0.7$ GeV, which was used in a number of previous calculations of single-pion production reactions [56, 64]. This value of $\tilde{\Lambda}$ is also consistent with the predictions of the lattice-QCD calculations [65, 66].

The detailed discussion on the choice of short-range cut-off parameters and their strong

[2] The cut-off parameters $\tilde{\Lambda}$ and $\tilde{\Lambda}_*$ in Eq. (25) were marked by a tilde sign to distinguish them from parameters used in a more familiar monopole vertex parameterization which follows from Eq. (25) when only pion is off-shell (see Ref. [47] for details).

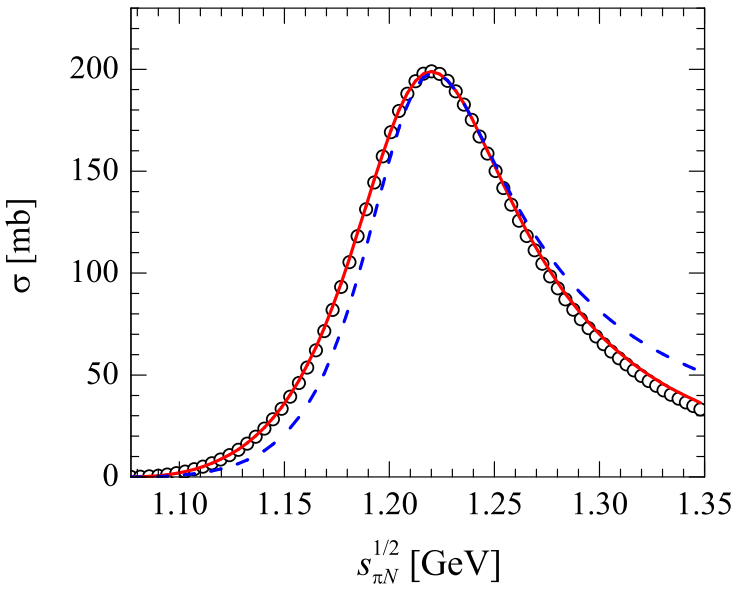

FIG. 2: The cross section of πN elastic scattering in the P_{33} partial wave. Solid and dashed lines show the calculations in the isobar model with the $\pi N\Delta$ vertex in the form (25) and cut-off parameters $\tilde{\Lambda}_* = 0.3$ and 0.52 GeV, respectively. Open circles correspond to the PWA data (SAID, solution WI08 [63]).

impact on cross sections of the $pp \to d\pi^+$ reaction can be found in our previous work [47]. It should be stressed here that the cut-off values chosen in our calculations are much lower than those traditionally used in the realistic NN-potential models. For example, in the Bonn model [67], the minimal values, which still allow a good description of NN-scattering phase shifts up to $T_N = 350$ MeV, are $\Lambda \simeq \Lambda_* \simeq 1.3$ GeV (in the CD-Bonn model [68] they are even higher). Such very high cut-off parameters apparently lead to increased meson-exchange contributions at short inter-nucleon distances. On the other hand, results of the numerous quark-model calculations agree, in general, that the parameters in meson-baryon vertices should be essentially soft, i.e., $\Lambda < 1$ GeV (see, e.g., [69] and references therein). In this case, one should seek for some alternative short-range mechanisms (such as formation of intermediate dibaryons) to describe the processes involving high momentum transfers within the two-nucleon system.

III. RESULTS FOR THE PARTIAL AND TOTAL CROSS SECTIONS

Here we calculated partial and total cross sections for the reaction $pp \to d\pi^+$ in the energy range $\sqrt{s} = 2.03$–2.27 GeV ($T_p \simeq 320$–860 MeV) using the above formalism. Three dibaryon resonances generated in pp channels ${}^1D_2$, ${}^3F_3$ and ${}^3P_2$ were included in calculations. At the present stage, we restricted ourselves to accurate description of three dominant partial-wave amplitudes and to qualitative estimation of dibaryon contributions in these amplitudes. We did not consider the possible dibaryons in small amplitudes (such as ${}^1G_4$, ${}^3P_1$, ${}^1S_0$, etc.), since the level of evidence for these dibaryons is less to date than for ${}^1D_2$, ${}^3F_3$ and ${}^3P_2$ ones, and also description of the small amplitudes would require a more precise treatment of the background meson-exchange processes. Besides that, increasing the number of dibaryons would increase the number of model parameters and thus complicate making reliable conclusions.

For consistency of our model, in calculations of conventional mechanisms ONE and $N\Delta$, we used the deuteron wave function (d.w.f.) derived in the dibaryon model for NN interaction [59, 60]. This d.w.f. has been truncated in the present study at high inter-nucleon momenta $p > 350$ MeV (with keeping the overall normalization) to prevent an unphysical rise of the differential cross section at large angles. So, the results obtained here with such regularized d.w.f. turned out to be very close to those with the conventional CD-Bonn d.w.f. [68].

Our model calculations were compared to the results of the most recent PWA (SAID, solution C500 [51, 63]), which is a coupled-channel analysis using $\pi^+ d \to pp$, $pp \to pp$ and $\pi^+ d \to \pi^+ d$ experimental data. The dibaryon parameters obtained by fitting the partial cross sections in three dominant partial waves ${}^1D_2P$, ${}^3F_3D$ and ${}^3P_2D$ to the PWA results are summarized in Table I. The relative phases φ between the resonance (dibaryon) and "background" (ONE + $N\Delta$) amplitudes were fixed as shown in the last column of the table (these values coincide with the best-fit results up to several degrees).

The dibaryon masses and widths obtained in our fit are generally consistent with the previous estimates [10, 70, 71]. It is particularly important that the parameters of the ${}^3P_2$ resonance found here are in a very good agreement with those found in a recent experimental work [24] from a global fit of experimental data on the differential cross section and proton analyzing power in the reaction $pp \to (pp)_0\pi^0$, i.e., $M_D = 2207 \pm 12$ and $\Gamma_D = 170 \pm 32$ MeV.

Nevertheless, in determining these parameters, one should bear in mind the possible uncertainties associated with our model assumptions as well as with different PWA results. Thus, two SAID PWA solutions, i.e., the coupled-channel solution C500 [51, 63] and the previous solution SP96 [63] for the $\pi^+ d \to pp$ reaction, give almost similar results for two dominating partial-wave amplitudes, but rather different results for the smaller $^3P_2 D$ amplitude at energies $\sqrt{s} > 2.17$ GeV — see Fig. 3. Our present fit for the latter amplitude gives some average result between these PWA solutions. Further, in view of a large width of the $^3P_2$ resonance, the extracted values of its parameters depend on the width parameterization used in the theoretical model. Thus, assuming the total width to be constant, we obtained for this resonance $M_D = 2162$ and $\Gamma_D = 154$ MeV. These values almost coincide with those found in [52] in the PWA of pp elastic scattering.

TABLE I: Parameters of dibaryon resonances used in calculations of the reaction $pp \to d\pi^+$. In the last column, the phases φ of the dibaryon production amplitudes with respect to the "background" (ONE + $N\Delta$) amplitude are shown.

$^{2S+1}L_J$	M_D (MeV)	Γ_D (MeV)	$\Gamma_i\Gamma_f$ (MeV^2)	α_{pp} (GeV)	$\Lambda_{\pi d}$ (GeV)	φ (deg)
$^1D_2$	2155	101	74	0.23	0.27	0
$^3F_3$	2197	152	53	0.32	0.53	0
$^3P_2$	2211	195	450	3.0	0.26	180

The results for the partial cross sections in three dominant partial waves are shown in the left panel of Fig. 3. The Argand plots for the respective amplitudes[3] are given in the right panel of Fig. 3.

As is seen from Fig. 3, the conventional mechanisms give approximately 40–50% of the cross sections in the partial waves $^1D_2 P$ and $^3F_3 D$. One should note that the initial- and final-state distortions which are not included in our model, would further decrease the calculated cross sections by about 20% [56]. On the other hand, the $N\Delta$ attraction generated by pion exchange can enhance the cross sections somehow [72]. We argue that this t-channel attraction which is governed by the cut-off parameters in the meson-baryon vertices should

[3] Note that due to a different normalization, partial-wave amplitudes defined in Sect. II should be multiplied by a factor $\sqrt{pq/s}/8\pi$ to be compared with the ones used in the SAID PWA [51].

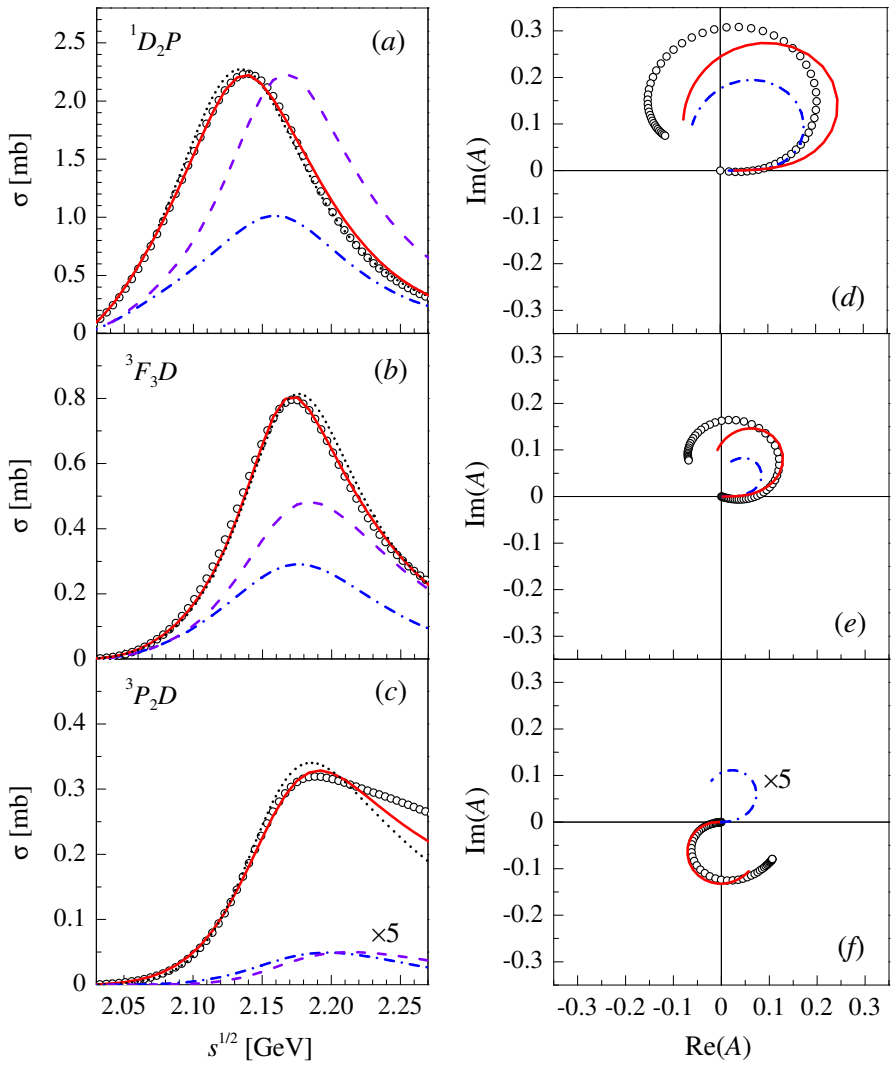

FIG. 3: Left panel: partial cross sections of the reaction $pp \to d\pi^+$ in the dominant partial waves ^1D_2P (a), ^3F_3D (b) and ^3P_2D (c). Right panel: Argand plots for the dominant partial-wave amplitudes ^1D_2P (d), ^3F_3D (e) and ^3P_2D (f). Dash-dotted lines show the summed contributions of two conventional mechanisms ONE + $N\Delta$ with a cut-off parameter $\tilde{\Lambda}_* = 0.3$ GeV consistent with πN elastic scattering (see Fig. 2). The contributions of ONE + $N\Delta$ mechanisms with an enhanced parameter $\tilde{\Lambda}_* = 0.52$ GeV are shown by dashed lines. The ONE + $N\Delta$ contributions in the ^3P_2D channel were multiplied by a factor of 5 for better visibility. Results of the full model calculations including also intermediate dibaryon resonances are shown by solid lines. The open circles and dotted lines correspond to the PWA results (SAID, solutions C500 and SP96, respectively [51, 63]).

be very moderate when using soft cut-off values, and the basic short-range attraction in the $N\Delta$ system would be induced in this case by generation of intermediate dibaryon resonances, similarly to that found for the NN system in the dibaryon model for NN interaction [59, 60]. Nevertheless, to examine possible effects of the $N\Delta$ t-channel interaction on the $pp \to d\pi^+$ cross sections, one could strengthen the intermediate Δ contribution through enhancing the cut-off parameter $\tilde{\Lambda}_*$ in the $\pi N\Delta$ vertex *ad hoc*. Thus, when enhancing $\tilde{\Lambda}_*$ from 0.3 to 0.52 GeV, one is able to reproduce the magnitude of the ${}^1D_2P$ partial cross section (see Fig. 3(a)). Note, however, that this worsens simultaneously the description of P_{33} πN elastic scattering (cf. Fig. 2). Further, as is shown in Fig. 3(b), the same cut-off parameter modification can also improve the description of the ${}^3F_3D$ partial cross section, though not enough to reproduce its empirical behavior.

On the other hand, in the ${}^3P_2D$ channel, the ONE + $N\Delta$ mechanisms give only ca. 2.5% of the partial cross section near the resonance peak, and this result very weakly depends on the $\pi N\Delta$ cut-off parameter value (see Fig. 3(c)). So that, the intermediate Δ excitation appears to play only a minor role in this channel. Besides that, the $N\Delta$ amplitude has an improper phase here (see Fig. 3(f)). So, the satisfactory description of the empirical data on the ${}^3P_2D$ partial cross section cannot be attained through any changes in parameters of the conventional mechanisms, and an additional resonance contribution appears to be urgently needed! The crucial role of proper description of the ${}^3P_2D$ partial-wave amplitude is particularly seen in the spin-correlation parameters, which will be discussed in the next section.

Here, we present also the results for the total cross section shown in Fig. 4. Though the conventional mechanisms reproduce a correct shape of the total cross section, the experimental data are underestimated by a factor of two, similarly to the partial cross sections in two dominant partial waves. Taking the intermediate dibaryons into account fills in the discrepancy between the conventional-model calculations and the data, thus leading to very good reproduction of experimental data in the whole energy range considered.

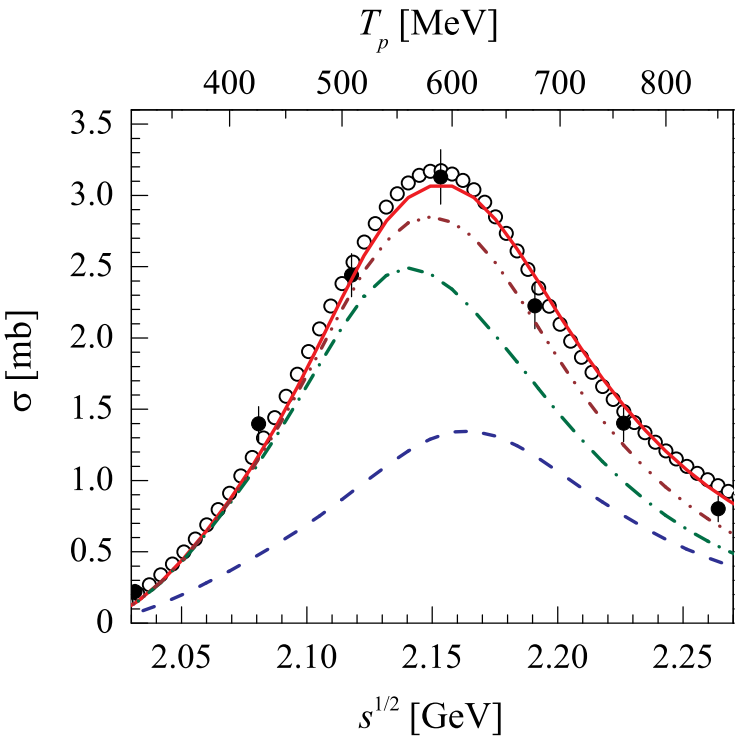

FIG. 4: Total cross section of the reaction $pp \to d\pi^+$. Dashed lines show the summed contributions of two conventional mechanisms ONE + $N\Delta$. Dash-dotted, dash-dot-dotted and solid lines correspond to the results of model calculations including also one ($^1D_2$), two ($^1D_2 + {}^3F_3$) and three ($^1D_2 + {}^3F_3 + {}^3P_2$) intermediate dibaryon resonances, respectively. Open circles correspond to PWA results (SAID, solution C500 [51, 63]) and filled circles — to the experimental data [73].

IV. RESULTS FOR DIFFERENTIAL CROSS SECTION AND POLARIZATION OBSERVABLES AT $T_p = 582$ MEV

In this section, the results for differential observables in the reaction $pp \to d\pi^+$ at energy $T_p = 582$ MeV ($\sqrt{s} = 2.15$ GeV) are presented. The energy value chosen here is close to that, where the total cross section has its maximum. Besides that, a rich set of experimental data exists in this energy region [74–78].

The results for the differential cross section are shown in Fig. 5. The differential cross section is described very well, except for the forward region, where high partial waves (giving a contribution less than 3% to the total cross section) obviously play an important role. Thus, one can see some underestimation of the contributions of these high partial waves in

our model. Further, the main contribution after the ^3P_2D channel comes from S-wave pion production in the ^3P_1S partial wave [50]. The S-wave pion production, which is important near the threshold, is usually described by some additional mechanism based on phenomenological Lagrangian approach [57]. Some contribution to this term comes also from S-wave πN scattering in the intermediate state. Both these mechanisms are not included in the present model. This is also the possible reason for a discrepancy between our calculation and experimental data for the proton analyzing power A_{y0} shown in Fig. 6(a). This observable is very sensitive to the small amplitudes in the non-dominant partial waves, and especially, to the ^3P_1S amplitude. In fact, just a few models were able to reproduce the shape of A_{y0} (see, e.g., [55, 56]). It is so sensitive to the tiny details of the model, that even the most accurate to date theoretical calculation based on solving exact Faddeev-type equations for the coupled $\pi NN \leftrightarrow NN$ system [54] could not reproduce its proper behavior. In particular, as was shown in [79], inclusion of the small S- and P-wave πN-scattering amplitudes just in first order leads to a proper description of the "double-hump" shape of A_{y0}, but the exact inclusion of these small amplitudes gives again an improper behavior like that shown in Fig. 6(a). So, even the qualitative description of A_{y0} requires an extremely accurate theoretical treatment of small partial-wave amplitudes.

We also calculated the deuteron vector analyzing power iT_{11} (see Fig. 6(b)). Its qualitative behavior is described properly already by conventional mechanisms, however, with a significant overestimation. Inclusion of dibaryon resonances, especially the $^3P_2$ one, allows to reduce the discrepancy with experimental data.

In general, one can conclude that our approximate model for conventional meson-exchange processes describe the experimental data for the basic observables not worse than more sophisticated theoretical models elaborated in previous years. The main difference is that we used soft values for the short-range cut-off parameters in meson-baryon vertices (*consistent with πN scattering*) and obtained lower cross sections, than other models which used larger cut-off values fitted ad hoc to describe the magnitude of the $pp \to d\pi^+$ cross section (see [54], Sect. III — "The off-shell modification"). Inclusion of dibaryon resonances is able to give the lacking short-range contributions to the cross sections and vector analyzing powers, however, without changing their qualitative behavior.

The quite opposite situation takes place with the spin-correlation parameters, the results for which are shown in Fig. 7. It is well-known that description of spin-correlation

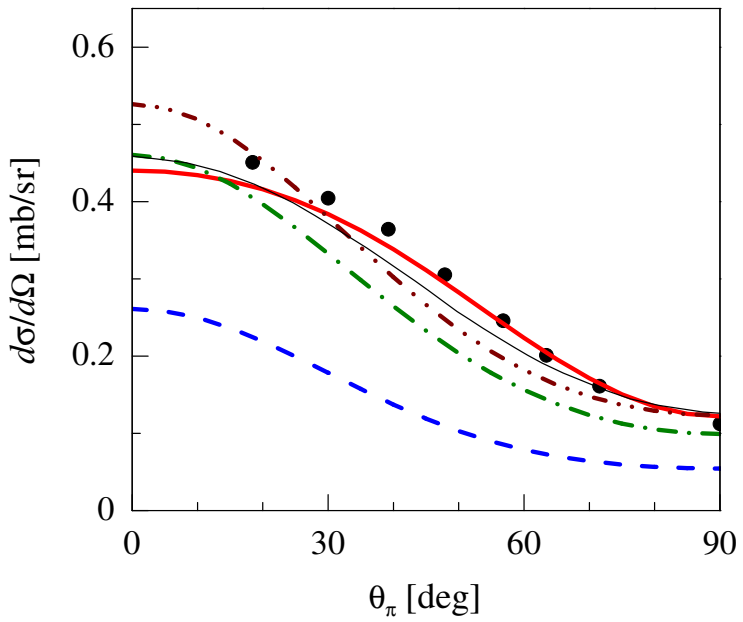

FIG. 5: Differential cross section in the reaction $pp \to d\pi^+$ at energy $T_p = 582$ MeV ($\sqrt{s} = 2.15$ GeV). The meaning of theoretical curves is the same as in Fig. 4. Thin solid line correspond to the conventional model calculations [54] including off-shell modifications and heavy-meson exchanges. Filled circles show the experimental data [74].

parameters in the $pp \to d\pi^+$ reaction was a serious problem for conventional theoretical models [54–56]. It was established long ago [56] that conventional meson-exchange mechanisms underestimate the contributions of triplet pp partial waves, which are very important for reproducing correctly the spin-correlation parameters. However, no definite solution for this problem has been found previously. As is seen from Fig. 7, just the ^3P_2D amplitude and its interference with other amplitudes changes strongly the qualitative behavior of the spin-correlation parameters, thus turning them into qualitative (or even semiquantitative) agreement with experimental data. And the proper magnitude of this amplitude can be obtained only by assuming a triplet P-wave dibaryon resonance excitation in addition to the conventional Δ excitation (see Figs. 3 (c) and (f)). This is likely *one of the most important results* of the present study.

In view of this result, we can suggest the possible reason for improper behavior of spin-correlation parameters in the model calculations [48, 49] which also included dibaryon resonances. Although the $^3P_2$ resonance was included in these calculations, its parameters

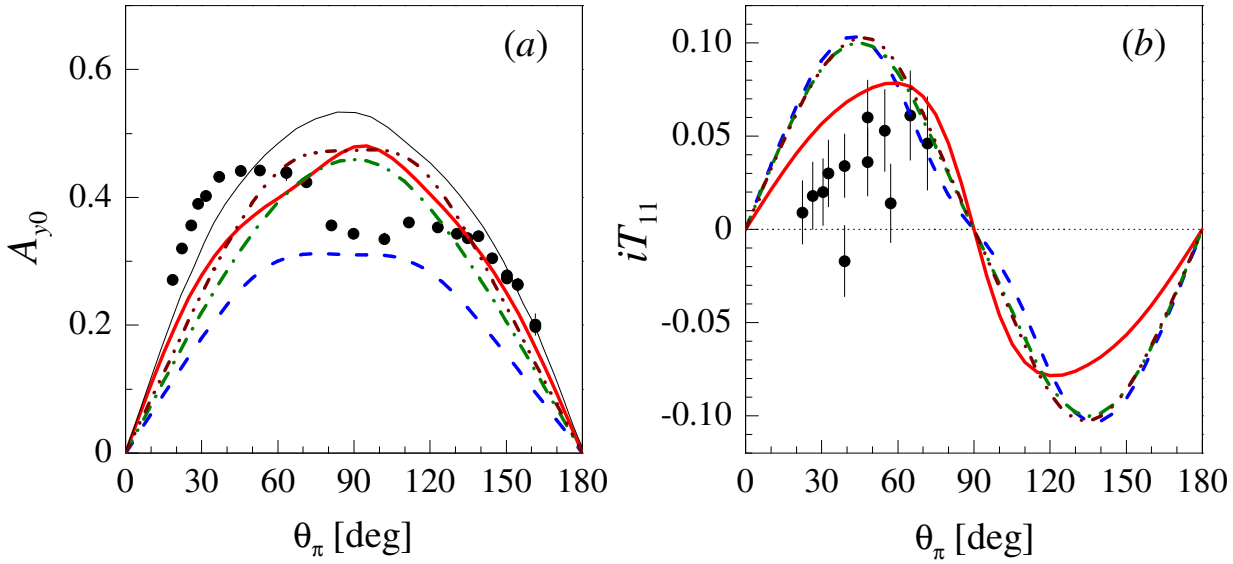

FIG. 6: Proton (a) and deuteron (b) vector analyzing powers in the reaction $pp \to d\pi^+$ at energy $T_p = 582$ MeV ($\sqrt{s} = 2.15$ GeV). The meaning of theoretical curves is the same as in Fig. 5. Filled circles show the experimental data [75] (a) and [76] (b). (The iT_{11} data [76] were obtained in an inverse process $\pi^+ d \to pp$ at $T_\pi = 140$ MeV, corresponding to $T_p = 562$ MeV.)

were not fitted individually, but together with parameters of the more intensive $^1D_2$ and $^3F_3$ resonances, to describe experimental data with mixed contributions of all resonances. As a result, its mass was found to be 2110 MeV and width 30 MeV, which are too low in comparison with experimental values and our results.

V. DISCUSSION AND SUMMARY

In the paper, we studied the manifestation of isovector dibaryon resonances $^1D_2$, $^3F_3$ and $^3P_2$ in the basic single-pion production reaction $pp \to d\pi^+$. All these resonances have been found in the PWA of pp elastic scattering [52, 53], however, the P-wave diproton resonance, being the least intensive, received less attention in literature than the D- and F-wave resonances. A new experimental evidence of the $^3P_2$ dibaryon has appeared just very recently [24] in the reaction $pp \to (pp)_0\pi^0$ where the more intensive $^1D_2$ and $^3F_3$ resonances are forbidden by angular momentum and parity conservation.

We have found the large effects of the $^3P_2$ diproton in the spin-correlation parameters of

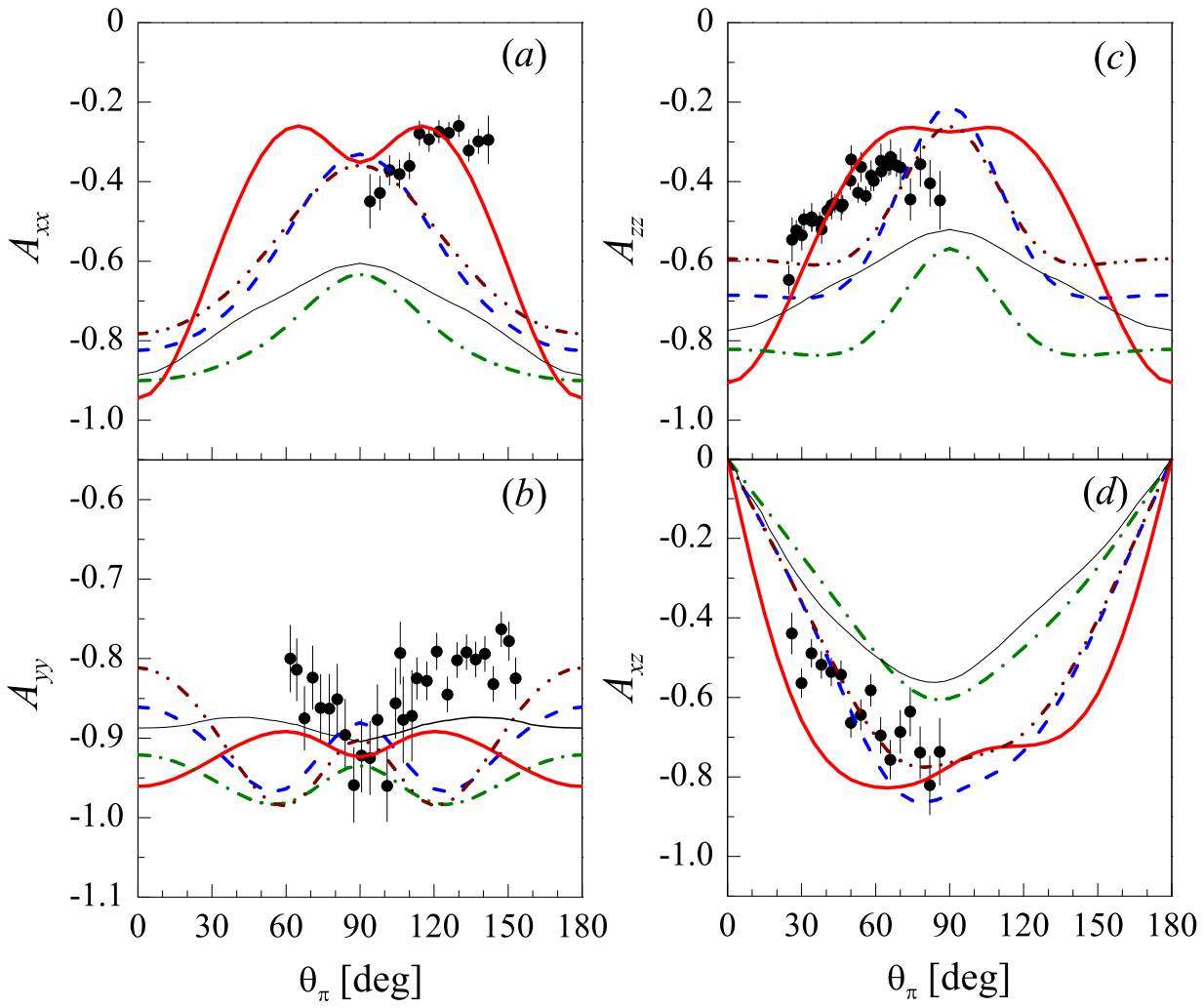

FIG. 7: Spin-correlation parameters A_{xx} (a), A_{yy} (b), A_{zz} (c), and A_{xz} (d) in the reaction $pp \to d\pi^+$ at energy $T_p = 582$ MeV ($\sqrt{s} = 2.15$ GeV). The meaning of theoretical curves is the same as in Fig. 5. Filled circles show the experimental data [77, 78] for $T_p = 578$ MeV.

the $pp \to d\pi^+$ reaction. In fact, the conventional models [54–56] (based mainly on the t-channel meson-exchange mechanisms) for this reaction generally resulted in underestimation and even improper behavior of the proton-proton spin-correlation parameters A_{xx}, A_{yy} and A_{zz}. We should note here that the coupled-channel approach of Niskanen [55] appeared to be more successful than other conventional models for $pp \to d\pi^+$ reaction, while still giving essential underestimation of A_{xx} and A_{yy}. However this approach turned out to completely fail for a similar reaction $pp \to (pp)_0\pi^0$, as was discussed in detail in a recent experimental paper [24]. Thus, the most recent experimental data in this area are in a strong

disagreement with the model predictions of Niskanen both in the forward cross section and in energy dependence. On the other hand, just these experimental data [24] revealed existence of the ${}^3P_2$ dibaryon. So, it is quite reasonable to suggest that the ${}^3P_2$ dibaryon which is clearly seen in the reaction $pp \to (pp)_0\pi^0$, should also manifest itself in a similar reaction $pp \to d\pi^+$, however, not in the unpolarized cross section where the dominant contributions are given by ${}^1D_2$ and ${}^3F_3$ dibaryons, but in more sensitive observables like spin-correlation parameters. In fact, we have shown that only assuming the contribution of the P-wave diproton resonance makes it possible to explain semi-quantitatively the experimental data for these observables. By the way, this explanation is rather similar to the explanation of the proton polarization in the reaction $d(\gamma,\vec{p})n$ at $E_\gamma = 400$–600 MeV found long ago in works [80, 81]. The strong disagreement for the outgoing proton polarization between the predictions of conventional models and experimental data [80] could only be explained by incorporation of the ${}^3D_3$ and ${}^3F_3$ intermediate dibaryon contributions. In this case one has another example of a process where the large spin-dependent observables could be explained only by assuming the intermediate dibaryon resonances.

Another interesting question worth to be discussed in connection with the P-wave diproton is a well-known puzzling behavior of the elastic NN-scattering phase shifts in the triplet P waves. In fact, while the triplet ${}^3P_0$ and ${}^3P_1$ NN phase shifts (and also the singlet one ${}^1P_1$) clearly demonstrate the short-range repulsive core behavior (with the core radius $r_c \simeq 0.9$ fm), the ${}^3P_2$ phase shifts are rising up to 600 MeV (lab.) and do not display any features of the repulsive core. However, in the conventional treatment of NN interaction, the short-range central-force repulsion should be a universal feature for all ${}^3P_J$, $J = 0, 1, 2$. The puzzle has been resolved in the conventional OBE-like models [82] through introduction of a highly intensive short-range spin-orbit force which produces a very strong attraction just in the ${}^3P_2$ channel and compensates completely the very large and broad repulsive core which is present in all P waves. This huge spin-orbit interaction looks rather unnatural and fitted *ad hoc* (for a detailed discussion of inconsistencies in the OBE-like NN-potential models see [83]).

The results of the present paper give some alternative explanation for the P-wave NN phase-shifts puzzle. In fact, one can think that the short-range ${}^3P_2$ dibaryon with a mass $M({}^3P_2) \simeq 2.2$ GeV induces as usually a strong NN attraction [59], the strongest at lab. energies $T_N \simeq 600$ MeV, so that, the above dibaryon-induced attraction at intermediate

energies can explain naturally the puzzling behavior of the ${}^3P_2$ NN phase shifts.

It is interesting to discuss further the possible quark structure of an isovector P-wave dibaryon and a mechanism of its decay with a pion emission. In the paper [47] we adopted the two-cluster $q^4 - q^2$ structure [84, 85] for the series of isovector dibaryons ${}^1D_2$, ${}^3F_3$, ${}^1G_4$, etc., with a tetraquark $q^4(S = 1, T = 0)$ and an axial diquark $q^2(S' = T' = 1)$ connected by a color QCD string with an orbital angular momentum $L_s = 0, 1, 2$, etc. The ${}^3P_2$ isovector dibaryon apparently does not belong to this series. If to assume the two-cluster $q^4 - q^2$ structure for this dibaryon as well, then the most appropriate structure would be a two-cluster state with a color string ($L_s = 1$) connecting the tetraquark $q^4(S = T = 1)$ and a scalar diquark $q^2(S' = T' = 0)$. However the tetraquark with $S = T = 1$ should be unstable against the decay into two (scalar and axial) diquarks. Then, two scalar diquarks resulted from such decay into the three-diquark system must be in a mutual P-wave due to the Pauli exclusion principle (see Fig. 8).

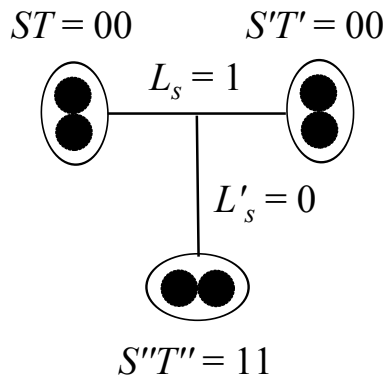

FIG. 8: Allowable three-diquark configuration for an isovector P-wave dibaryon.

The "natural" decay of the three-diquark state with a pion emission, viz. $q^2(S'' = T'' = 1) \to q^2(S'' = T'' = 0)$ and $L'_s = 0 \to L'_s = 1$ is unlikely because the final state in this case would be the so-called "demon deuteron" [86] with two P-wave strings, which would have a higher mass than the initial P-wave dibaryon. Thus, the most probable transition should be the rearrangement of the three-cluster configuration shown in Fig. 8 to a conventional two-cluster $q^3 - q^3$ state with a P-wave string between two $3q$ clusters. Then this state, in its turn, decays via a single-pion emission to the final deuteron ($S = 1, T = 0$) or singlet deuteron ($S = 0, T = 1$), i.e., by the usual spin-flip or isospin-flip transitions.

The recent experiment [24] revealed existence of the ${}^3P_0$ dibaryon resonance, along with

the $^3P_2$ one. Besides that, the recent *pp*-scattering analysis [87] predicts three diproton resonances ^3P_J, $J = 0, 1, 2$. The decay of the $^3P_0$ resonance into $d\pi^+$ channel is forbidden due to angular momentum and parity conservation, but it can decay into $(pp)_0\pi^0$ channel. For the same reasons, the $^3P_1$ resonance can decay into $d\pi^+$, but not into $(pp)_0\pi^0$ channel. If the $^3P_0$ and/or $^3P_1$ dibaryons really exist, all the above quark-structure consideration will hold for them either. However, these resonances obviously give a very small contribution to NN elastic scattering (compared to the background meson-exchange mechanisms), which is indicated by a very moderate attraction in the $^3P_0$ channel and an almost negligible attraction in the $^3P_1$ channel (compared to the strong attraction in the $^3P_2$ channel — see the above discussion of the P-wave phase-shifts puzzle). Furthermore, these resonances, contrary to the $^3P_2$ dibaryon, were not found in most phase-shift analyses of *pp* elastic scattering. So, further studies are needed to shed light on existence and properties of the P-wave diproton resonances.

To summarize, we have shown that intermediate dibaryon resonances in the NN channels $^1D_2$, $^3F_3$ and $^3P_2$ are very likely to be responsible for a significant part of the cross sections of the basic single-pion production process $pp \to d\pi^+$ in a broad energy range (T_p = 400–800 MeV). Moreover, the $^3P_2$ diproton resonance has been shown to be responsible for the most important characteristic features of the *pp* spin-correlation parameters in this reaction (at least near $T_p \simeq 600$ MeV). So, the role of the isovector dibaryons in single-pion production in *pp* collisions is rather similar to that of the isoscalar $^3D_3$ dibaryon in double-pion production in *pn* collisions [20, 88]. Besides that, the isovector dibaryons might play an important role also in double-pion production in *pp* collisions [47]. These results may have many far-going implications in hadronic and nuclear physics.

ACKNOWLEDGEMENTS

The work was done under partial financial support from RFBR grants Nos. 16-02-00049, 16-02-000265 and 16-52-12005. M.N.P. also appreciates support from Dynasty Foundation.

[1] R. L. Jaffe, Phys. Rev. Lett. **38**, 195 (1977).

[2] A. T. M. Aerts, P. J. G. Mulders, and J. J. de Swart, Phys. Rev. D **17**, 260 (1978).

[3] V. A. Matveev and P. Sorba, Nuovo Cim. **A45**, 257 (1978).

[4] I. P. Auer et al., Phys. Lett. **B70**, 475 (1977).

[5] I. P. Auer et al., Phys. Rev. Lett. **41**, 1436 (1978).

[6] E. K. Biegert et al., Phys. Lett. **B73**, 235 (1978).

[7] I. P. Auer et al., Phys. Rev. Lett. **48**, 1150 (1982).

[8] I. P. Auer et al., Phys. Rev. Lett. **62**, 2649 (1989).

[9] M. P. Locher, M. E. Sainio, and A. Svarc, Adv. Nucl. Phys. **17**, 47 (1986).

[10] R. Bhandari, R. A. Arndt, L. D. Roper, and B. J. VerWest, Phys. Rev. Lett. **46**, 1111 (1981).

[11] R. A. Arndt, L. D. Roper, R. L. Workman, and M. W. McNaughton, Phys. Rev. D **45**, 3995 (1992).

[12] A. V. Kravtsov, M. G. Ryskin, and I. I. Strakovsky, J. Phys. G **9**, L187 (1983).

[13] I. I. Strakovsky, A. V. Kravtsov, and M. G. Ryskin, Sov. J. Nucl. Phys. **40**, 273 (1984).

[14] N. Hoshizaki, Prog. Theor. Phys. **60**, 1796 (1978).

[15] N. Hoshizaki, Prog. Theor. Phys. **61**, 129 (1979).

[16] Y. A. Simonov and M. van der Velde, J. Phys. G **5**, 493 (1979).

[17] J. A. Niskanen, Phys. Lett. **B112**, 17 (1982).

[18] I. I. Strakovsky, AIP Conf. Proc. **221**, 218 (1991).

[19] A. Valcarce, H. Garcilazo, R. D. Mota, and F. Fernandez, J. Phys. G **27**, L1 (2001).

[20] P. Adlarson et al. (WASA-at-COSY Collaboration), Phys. Rev. Lett. **106**, 242302 (2011).

[21] P. Adlarson et al. (WASA-at-COSY Collaboration, SAID Data Analysis Center), Phys. Rev. Lett. **112**, 202301 (2014).

[22] J. T. Goldman, K. Maltman, G. J. Stephenson, K. E. Schmidt, and F. Wang, Phys. Rev. C **39**, 1889 (1989).

[23] F. J. Dyson and N.-H. Xuong, Phys. Rev. Lett. **13**, 815 (1964).

[24] V. I. Komarov et al., Phys. Rev. C **93**, 065206 (2016).

[25] A. Gal and H. Garcilazo, Phys. Rev. Lett. **111**, 172301 (2013).

[26] A. Gal and H. Garcilazo, Nucl. Phys. **A928**, 73 (2014).

[27] M. Bashkanov, S. J. Brodsky, and H. Clement, Phys. Lett. **B727**, 438 (2013).

[28] H. Huang, J. Ping, and F. Wang, Phys. Rev. C **89**, 034001 (2014).

[29] Y. Dong, P. Shen, F. Huang, and Z. Zhang, Phys. Rev. C **91**, 064002 (2015).

[30] S. J. Brodsky, C.-R. Ji, and G. P. Lepage, Phys. Rev. Lett. **51**, 83 (1983).

[31] S. J. Brodsky and C.-R. Ji, Phys. Rev. D **33**, 1406 (1986).

[32] CERN Courier **54**, 6 (2014), URL `http://cerncourier.com/cws/article/cern/57836`.

[33] A. I. Baz', Adv. Phys. (Phil. Mag. Suppl.) **8**, 349 (1959).

[34] E. P. Wigner, Phys. Rev. **73**, 1002 (1948).

[35] V. I. Serov and V. A. Zhmailo, Sov. Phys. JETP **17**, 227 (1963).

[36] F. Ajzenberg-Selove and T. Lauritsen, Nucl. Phys. **11**, 1 (1959).

[37] C. Hanhart, Yu. S. Kalashnikova, and A. V. Nefediev, Phys. Rev. D **81**, 094028 (2010).

[38] T. Hyodo, Phys. Rev. Lett. **111**, 132002 (2013).

[39] R. A. Arndt, J. M. Ford, and L. D. Roper, Phys. Rev. D **32**, 1085 (1985).

[40] K. A. Olive et al. (Particle Data Group), Chin. Phys. C **38**, 090001 (2014), URL `http://pdg.lbl.gov`.

[41] A. V. Sarantsev et al., Phys. Lett. **B659**, 94 (2008).

[42] T. Skorodko et al., Eur. Phys. J. **A35**, 317 (2008).

[43] I. T. Obukhovsky, A. Faessler, D. K. Fedorov, T. Gutsche, and V. E. Lyubovitskij, Phys. Rev. D **84**, 014004 (2011).

[44] A. Gal, Acta Phys. Polon. **B47**, 471 (2016).

[45] R. Aaij et al. (LHCb Collaboration), Phys. Rev. Lett. **112**, 222002 (2014).

[46] R. Aaij et al. (LHCb Collaboration), Phys. Rev. Lett. **115**, 072001 (2015).

[47] M. N. Platonova and V. I. Kukulin, Nucl. Phys. **A946**, 117 (2016).

[48] H. Kamo and W. Watari, Prog. Theor. Phys. **62**, 1035 (1979).

[49] H. Kamo and W. Watari, Prog. Theor. Phys. **64**, 338 (1980).

[50] R. A. Arndt, I. I. Strakovsky, R. L. Workman, and D. V. Bugg, Phys. Rev. C **48**, 1926 (1993).

[51] C.-H. Oh, R. A. Arndt, I. I. Strakovsky, and R. L. Workman, Phys. Rev. C **56**, 635 (1997).

[52] R. A. Arndt, J. S. Hyslop, III, and L. D. Roper, Phys. Rev. D **35**, 128 (1987).

[53] Y. Higuchi, N. Hoshizaki, H. Masuda, and H. Nakao, Prog. Theor. Phys. **86**, 17 (1991).

[54] G. H. Lamot, J. L. Perrot, C. Fayard, and T. Mizutani, Phys. Rev. C **35**, 239 (1987).

[55] J. A. Niskanen, Phys. Lett. **B141**, 301 (1984).

[56] W. Grein, A. König, P. Kroll, M. P. Locher, and A. Švarc, Ann. Phys. **153**, 301 (1984).

[57] M. Brack, D. O. Riska, and W. Weise, Nucl. Phys. **A287**, 425 (1977).

[58] M. Jacob and G. C. Wick, Ann. Phys. **7**, 404 (1959).

[59] V. I. Kukulin, I. T. Obukhovsky, V. N. Pomerantsev, and A. Faessler, J. Phys. G **27**, 1851

(2001).

[60] V. I. Kukulin, I. T. Obukhovsky, V. N. Pomerantsev, and A. Faessler, Int. J. Mod. Phys. **E11**, 1 (2002).

[61] J. D. Jackson, Nuovo Cim. **34**, 1644 (1964).

[62] V. V. Anisovich, E. M. Levin, A. K. Likhoded, and Y. G. Stroganov, Sov. J. Nucl. Phys. **8**, 339 (1969).

[63] The SAID partial-wave analysis website. (2016), URL `http://gwdac.phys.gwu.edu/`.

[64] O. Imambekov and Y. N. Uzikov, Sov. J. Nucl. Phys. **47**, 695 (1988).

[65] K. F. Liu et al., Phys. Rev. D **59**, 112001 (1999).

[66] G. Erkol, M. Oka, and T. T. Takahashi, Phys. Rev. D **79**, 074509 (2009).

[67] R. Machleidt, K. Holinde, and C. Elster, Phys. Rept. **149**, 1 (1987).

[68] R. Machleidt, Phys. Rev. C **63**, 024001 (2001).

[69] W. Koepf, L. L. Frankfurt, and M. Strikman, Phys. Rev. D **53**, 2586 (1996).

[70] N. Hoshizaki, Prog. Theor. Phys. **89**, 251 (1993).

[71] A. Yokosawa, Int. J. Mod. Phys. A **05**, 3089 (1990).

[72] J. A. Niskanen and P. Wilhelm, Phys. Lett. **B359**, 295 (1995).

[73] F. Shimizu et al., Nucl. Phys. **A386**, 571 (1982).

[74] J. Hoftiezer et al., Nucl. Phys. **A402**, 429 (1983).

[75] J. Hoftiezer et al., Nucl. Phys. **A412**, 286 (1984).

[76] G. R. Smith et al., Phys. Rev. C **30**, 980 (1984).

[77] E. Aprile et al., Nucl. Phys. **A379**, 369 (1982).

[78] E. Aprile et al., Nucl. Phys. **A415**, 365 (1984).

[79] T. Mizutani, C. Fayard, G. H. Lamot, and R. S. Nahabetian, Phys. Lett. **B107**, 177 (1981).

[80] T. Kamae et al., Phys. Rev. Lett. **38**, 468 (1977).

[81] T. Kamae and T. Fujita, Phys. Rev. Lett. **38**, 471 (1977).

[82] A. Bohr and B. R. Mottelson, *Nuclear structure*, vol. I (World Scientific, Singapore, 1999).

[83] V. I. Kukulin and M. N. Platonova, Phys. At. Nucl. **76**, 1465 (2013).

[84] P. J. Mulders, A. T. M. Aerts, and J. J. De Swart, Phys. Rev. D **21**, 2653 (1980).

[85] L. A. Kondratyuk, B. V. Martemyanov, and M. G. Shchepkin, Sov. J. Nucl. Phys. **45**, 776 (1987).

[86] S. Fredriksson and M. Jändel, Phys. Rev. Lett. **48**, 14 (1982).

[87] G. Papadimitriou and J. P. Vary, Phys. Lett. **B746**, 121 (2015).

[88] M. N. Platonova and V. I. Kukulin, Phys. Rev. C **87**, 025202 (2013).